

# Vision-Based Vehicle Trajectory Following with Constant Time Delay

Hien K. Goi, Timothy D. Barfoot, Bruce A. Francis, and Jared L. Giesbrecht

**Abstract.** A convoy problem is formulated and solved for two four-wheeled vehicles. The task is for the second vehicle to follow the leader's trajectory with a constant time delay. This delayed trajectory can be viewed as the trajectory of a *delayed leader*. This novel constant-time-delay concept allows for the estimation of the delayed leader's speed and heading using the vehicle kinematics. Decoupled longitudinal and lateral controllers are developed based on the constant-time-delay approach. The lateral controller includes a look-ahead feature to compensate for steering delays. Successful field trials were conducted with full-sized military vehicles on a 1.3-kilometre test track. The tracking errors from differential global positioning system (DGPS) ground truth covering 13 kilometres are presented.

## 1 Introduction

Motivating our research is a military scenario in which a vehicle convoy traverses hostile territory to deliver supplies. Naturally, equipping every vehicle in the convoy with armour that will protect its occupants is expensive. To reduce the cost, autonomous unarmoured supply vehicles may be used, whereby each autonomous

---

Hien K. Goi and Bruce A. Francis

Department of Electrical and Computer Engineering, University of Toronto  
Toronto, Ontario, Canada

e-mail: [hien.goi@utoronto.ca](mailto:hien.goi@utoronto.ca), [bruce.francis@utoronto.ca](mailto:bruce.francis@utoronto.ca)

Timothy D. Barfoot

University of Toronto Institute for Aerospace Studies  
Toronto, Ontario, Canada  
e-mail: [tim.barfoot@utoronto.ca](mailto:tim.barfoot@utoronto.ca)

Jared L. Giesbrecht

Defence Research and Development Canada-Suffield  
Medicine Hat, Alberta, Canada  
e-mail: [jared.giesbrecht@drdc-rddc.gc.ca](mailto:jared.giesbrecht@drdc-rddc.gc.ca)

vehicle would follow the trajectory of the vehicle ahead of it. To follow the vehicle ahead, an autonomous vehicle can sometimes take advantage of a global positioning system (GPS), inter-vehicle communications, and/or lane markers/magnets. However, since the vehicle convoy is in hostile territory, GPS signals may be jammed, inter-vehicle communications may be intercepted, the roads may be unstructured.

Based on this motivating example, our project goal is to design and test a control system to allow a convoy of full-sized autonomous vehicles with large inter-vehicle spacing to follow the lead vehicle's trajectory without cutting corners on turns. The control system should use only on-board sensors, avoiding the use of GPS, inter-vehicle communications, and lane markers/magnets. This paper reports our preliminary experimental results performed on two full-sized vehicles where the leader vehicle is manually driven and the follower vehicle is autonomously controlled. In our field trials to date, we do not use lane marker/magnets or radio communications between vehicles. However, we do use GPS to measure the follower's position due to a poor odometry system.

To our knowledge, there have been only a few prior experimental works relevant to our project goal. The most relevant is Gehrig and Stein [4], who tested a path-following strategy that, with the addition of autonomous speed control, could potentially follow the leader's trajectory at large distances without cutting corners. Their 'Control Using Trajectory' (CUT) algorithm stores the time history of the leader's path and steers towards the leader's position that is a constant distance ahead of the follower's current position. Although Gehrig and Stein's experiments showed improvements in tracking the leader's path over a system without CUT, the experimental data was limited to less than 15 seconds.

Other experimental works that use only on-board sensors include Benhimane et al. [1], Franke et al. [3], and Kehtarnavaz et al. [6]. Benhimane et al. developed a vehicle-following system with the objective of tracking a virtual leader a constant distance behind the leader. However, since the trajectory of the leader is not stored, the follower may cut corners on turns. Furthermore, their experimental data was limited to 2 minutes, and the maximum follower speed was 1 m/s. Both Franke et al. and Kehtarnavaz et al. had vehicle-following systems that were based on the follower's range and bearing to the leader. As such, both implemented steering controls that simply steered toward the leader. Such steering controls are known to deviate from the leader's path [4].

Daviet and Parent [2] also performed vehicle-following experiments without using inter-vehicle communications. Their vehicles travelled up to 10 m/s, but the corresponding distance separation was only 4.5 metres, and the experimental data shown was for only 30 seconds. They also used the strategy of simply steering towards the leader, but they do suggest storing the leader's trajectory in a future implementation. Although Schneiderman et al. [8] used radio communications, the radio link was used to interact with the follower's computer system. They demonstrated a path-following system with a 33-kilometre traverse at speeds of 13.9 to 20.8 m/s and at following distances of 5 to 15 metres. However, only the steering was autonomous, and the follower did not store the leader's path.

## 1.1 Problem Formulation

To meet our project goal, we take a novel approach to tracking the leader's trajectory. Our objective is for the follower to track the planar trajectory of the leader delayed by a constant time,  $\tau$ . Specifically, if  $(x(t), y(t))$  is the position of the follower with respect to an inertial frame and  $(x_0(t), y_0(t))$  is the position of the leader with respect to the same frame, then we want  $(x(t), y(t))$  to track  $(x_0(t - \tau), y_0(t - \tau))$ . For brevity, we define the delayed leader position,  $(x_0(t - \tau), y_0(t - \tau))$ , as  $(x_d(t), y_d(t))$ . The leader, delayed leader, and follower are shown in Fig. 1a. It is important to note that our definition is different from the constant time headway [9] definition. The tracking error in our definition is with respect to the leader's delayed position, while the tracking error in constant time headway is with respect to the leader's current position.

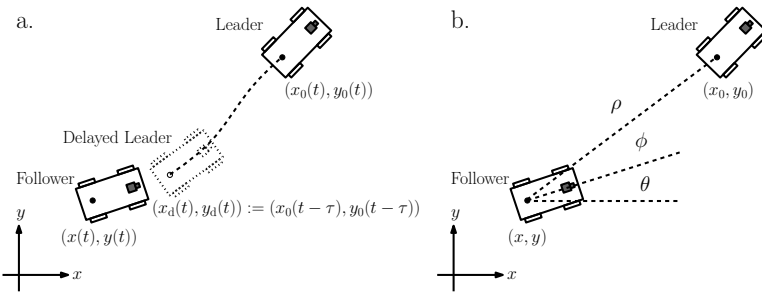


**Fig. 1** (a) Leader, delayed leader, and follower in an inertial frame. (b) The leader's and follower's positions are related by the follower's heading,  $\theta$ , and the range,  $\rho$ , and bearing,  $\phi$ , to the leader.

There are two main advantages to our approach: 1) tracking the delayed leader provides us with ‘future’ delayed-leader positions since we have measurements up to the leader’s current position; and 2) the following distance varies based on the leader’s speed. The first advantage allows us to track the leader’s trajectory without having to measure the leader’s speed or heading. Instead, the delayed leader’s speed and heading are estimated using the delayed leader’s future positions. Having future position measurements also allows our system to use interpolation to handle the occasional data dropout, which is to be expected with a vehicle-following system on bumpy roads. Due to space limitations, the details of our interpolation technique are not discussed in this paper. The second advantage naturally causes the following distance to be smaller when the leader slows down on difficult portions of the road, e.g., turns and rough terrain. The smaller following distance allows for more accurate measurements of the leader’s position, which will help the tracking during those difficult portions.

## 2 System Architecture and Design

Given the problem formulation, the follower requires a means to localize its position,  $(x, y)$ , and heading,  $\theta$ , relative to an inertial frame. This localization can be done using GPS or wheel odometry. Since the convoy is to operate in hostile territory, our preference is to use wheel odometry. To measure the leader's relative position, we use a pan-tilt-zoom monocular camera system with a colour tracker to servo around a coloured target on the back of the leader [5]. Knowing the offsets between the camera and the follower's rear axle and between the target and the leader's rear axle, we can obtain the range,  $\rho$ , and bearing,  $\phi$ , to the leader from the camera's output, as shown in Fig. 1b.

A top level diagram of our vehicle control system is shown in Fig. 2. The camera system outputs the range and bearing to the leader. The odometry measures the follower's speed and steering,  $(v, \gamma)$ , and provides estimates of the follower's position and heading,  $(\hat{x}, \hat{y}, \hat{\theta})$ . The range, bearing, and odometric estimates are fed into a nonlinear observer to produce estimates of the delayed leader's position, heading, and speed,  $(\hat{x}_d, \hat{y}_d, \hat{\theta}_d, \hat{v}_d)$ , along with estimates of a look-ahead point's position and heading,  $(\hat{x}_l, \hat{y}_l, \hat{\theta}_l)$ . These estimates are used by the control laws to produce the commanded speed and steering,  $(v_c, \gamma_c)$ , which are the inputs to the follower. The details of the vehicle model for the follower, the control laws, and the nonlinear observer are provided in the following subsections.

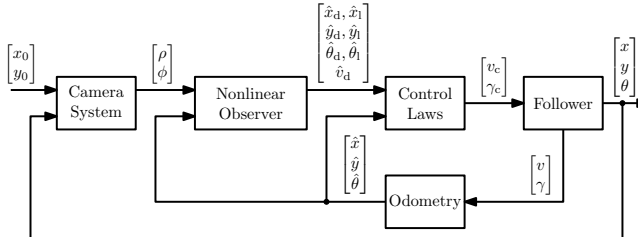


**Fig. 2** Top level diagram of vehicle control system.

### 2.1 Follower Vehicle Model

For the vehicle kinematics, we chose the bicycle model, which is given by

$$\dot{x} = v \cos \theta, \quad \dot{y} = v \sin \theta, \quad \dot{\theta} = \frac{v}{d} \tan \gamma,$$

where  $(x, y)$  is the position of the rear axle,  $\theta$  is the vehicle's heading,  $d$  is the distance between the front and rear axles,  $v$  is the vehicle's speed, and  $\gamma$  is the vehicle's steering angle. We derived a local linear model by examining the longitudinal and lateral tracking errors,  $(e_1, e_2)$ , in the follower's frame. The tracking errors are defined to be

$$\begin{bmatrix} e_1 \\ e_2 \end{bmatrix} := \begin{bmatrix} \cos \theta & \sin \theta \\ -\sin \theta & \cos \theta \end{bmatrix} \begin{bmatrix} x_d - x \\ y_d - y \end{bmatrix}.$$

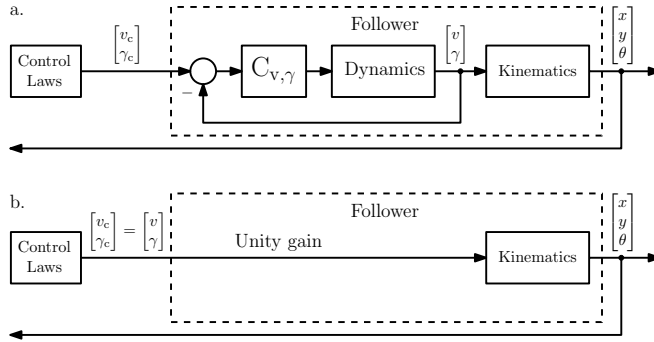


**Fig. 3** (a) Inner/outer loop architecture for the follower. (b) The outer-loop controller is designed by assuming the inner loop is a unity gain.

Linearizing the tracking errors and the bicycle model along a constant-velocity trajectory, we obtain a local kinematic model for the follower given by

$$\dot{e}_1 = v_d - v, \quad \dot{e}_2 = v_d e_3, \quad \dot{e}_3 = -\frac{v_d}{d} \gamma,$$

where  $v_d$  is the speed of the delayed leader and  $e_3 := \theta_d - \theta$  is the heading error.

For the vehicle dynamics, we assume the follower has an inner-loop controller,  $C_{v,\gamma}$ , that stabilizes its throttle and steering dynamics<sup>1</sup>. This assumption creates an inner/outer loop architecture where  $C_{v,\gamma}$  stabilizes the vehicle dynamics in the inner loop and our controller controls the vehicle kinematics in the outer loop, as shown in Fig. 3.

A common practice with the above architecture is to design the outer-loop controller by treating the inner loop as a unity gain [7]. This assumption works well if the gains of the outer-loop controller are kept low enough such that the bandwidth of the outer loop is approximately 5 to 10 times smaller than the bandwidth of the inner loop. As a result, the kinematic model of the follower is

$$\dot{e}_1 = v_d - v_c, \quad \dot{e}_2 = v_d e_3, \quad \dot{e}_3 = -\frac{v_d}{d} \gamma_c. \quad (1)$$

In our implementation, we validated the bandwidth separation between our inner and outer loops through simulation and through the actual tuning of the gains in experimental trials.

## 2.2 Control Laws

Since the longitudinal and lateral directions of (1) are decoupled, it can be shown that choosing

---

<sup>1</sup> This was the case for the vehicles that we employed.

$$\begin{aligned} v_c &= v_d + k_{p,1}e_1, \quad k_{p,1} > 0 \\ \gamma_c &= k_{p,2}e_2 + k_{p,3}e_3, \quad k_{p,2}, k_{p,3} > 0 \end{aligned}$$

will regulate the tracking errors to zero for the linearized model.

After some initial field trials, we discovered that the follower was turning late, which caused a large lateral error. We hypothesized that the late turning was caused by the low gains in our controller and the delays in the vehicle's steering dynamics. To compensate, we added a look-ahead feature for the lateral controller. We define the look-ahead point as

$$(x_l(t), y_l(t)) := (x_0(t - \tau + l), y_0(t - \tau + l)), \quad 0 \leq l \leq \tau,$$

where  $l$  is a constant look-ahead time. With a look-ahead time defined, the lateral and heading errors are computed by

$$e_2 = -(x_l - x) \sin \theta + (y_l - y) \cos \theta, \quad e_3 = \theta_l - \theta,$$

where  $\theta_l$  is the heading of the look-ahead point.

### 2.3 Nonlinear Observer

From the control laws, it is obvious that we need estimates of the tracking and heading errors,  $(e_1, e_2, e_3)$ , and the delayed leader's speed,  $v_d$ . The tracking and heading errors are calculated from the state of the follower,  $(x, y, \theta)$ , the state of the delayed leader,  $(x_d, y_d, \theta_d)$ , and the state of the look-ahead point,  $(x_l, y_l, \theta_l)$ . The delayed leader's speed can be calculated from the delayed leader's instantaneous change in position,  $(\dot{x}_d, \dot{y}_d)$ .

The follower's odometry provides an estimate of its state. The delayed leader's position is simply the leader's current position delayed by  $\tau$ . From Fig. 1b, the leader's position can be computed by

$$x_0 = x + \rho \cos(\phi + \theta), \quad y_0 = y + \rho \sin(\phi + \theta).$$

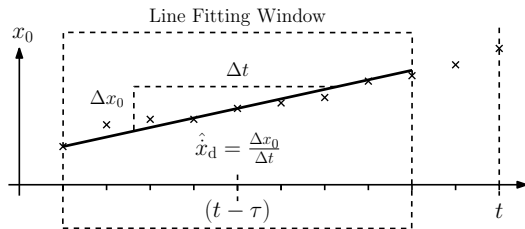
We use a data buffer to emulate the constant time delay in our implementation. The position of the look-ahead point is calculated in the same manner.

From the bicycle kinematics, the delayed leader's speed and heading can be calculated by

$$v_d = \sqrt{\dot{x}_d^2 + \dot{y}_d^2}, \quad \theta_d = \text{atan2}(\dot{y}_d, \dot{x}_d).$$

We obtain an estimate of  $\dot{x}_d$  by fitting a line to an  $n$ -second window of  $x_0$  measurements centred around  $t - \tau$ , where  $n$  is configurable and a multiple of the data rate for  $x_0$ . A depiction is shown in Fig. 4, where the line is fitted using least squares. The slope of the line is then used as the estimate of  $\dot{x}_d$ . The estimate of  $\dot{y}_d$  is obtained in the same manner, thus allowing us to calculate  $\hat{\theta}_d$ . A similar approach is used to estimate the look-ahead point's heading. Plots of the estimated and actual

**Fig. 4** Estimating  $\dot{x}_d$  using a line fitting window centred around  $t - \tau$ . The window size is  $n$  seconds, where  $n$  is configurable and a multiple of the data rate for  $x_0$ . The line is fitted using least squares, and the slope of the line is used as the estimate of  $\dot{x}_d$ .



delayed leader's speeds and headings during a field trial are given in the next section to validate this windowing technique.

### 3 Field Trials

Field trials were conducted at Defence Research and Development Canada (DRDC)-Suffield, Alberta, Canada, in November, 2008, with two MultiAgent Tactical Sentry (MATS) vehicles. A picture of the MATS leader vehicle is shown in Fig. 5. The coloured target is used by the follower's camera system to measure the range and bearing to the leader. Each MATS vehicle is equipped with an on-board computer, a pan-tilt-zoom monocular camera, a GPS antenna, and a data link to a ground station to receive DGPS corrections. The DGPS data serves to provide ground truth for the trials. Each MATS is also equipped with odometric sensors that provide the vehicle's current speed and steering angle.

The test track is a 1.3-kilometre loop shown in Fig. 6. The track is a gravel road and is approximately 7 metres wide. The most difficult portion of the track is the 60-degree hairpin turn located at the north-west corner of the track.

#### 3.1 Odometry Localization

Tracking the delayed leader using odometry localization proved to be difficult with the follower's current odometric sensors. The problem stemmed from an encoder

**Fig. 5** The MATS leader vehicle. The coloured target is used by the follower's camera system to measure the range and bearing to the leader. Each MATS vehicle is equipped with an on-board computer, a pan-tilt-zoom monocular camera, a GPS antenna, and a data link to a ground station to receive DGPS corrections.

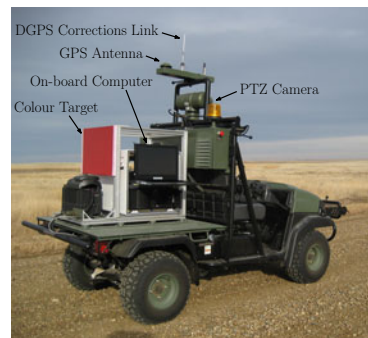
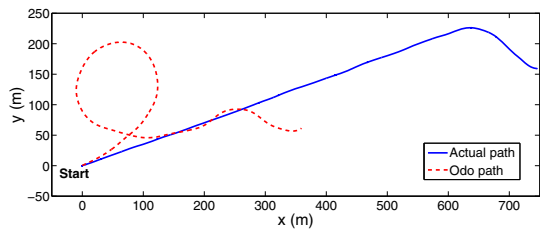


**Fig. 6** The 1.3-kilometre test track used for field trials. The track is a gravel road and is approximately 7 metres wide. The most difficult portions of the track are the U-turn and the hairpin turn.



**Fig. 7** The follower's actual path in comparison with its path estimated from odometric sensors. A crowned road caused the odometry to produce a circular path estimate when the follower was actually traveling straight.



located on the steering column used to measure the steering angle. Since there was significant ‘play’ between the steering wheel and the front wheels, the steering measurement did not accurately represent the angle of the front wheels and was highly sensitive to road slope. As a result, the follower’s heading estimate was very inaccurate, resulting in poor path estimates. An example is shown in Fig. 7, when tracking with odometry localization was performed off the test track. In this case, a crowned road caused the odometry to produce a circular path estimate when the follower was actually traveling straight.

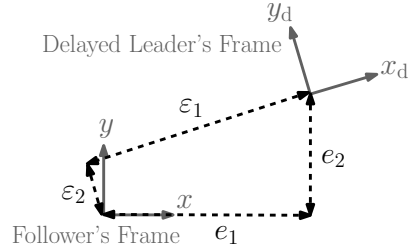
### 3.2 DGPS Localization

Using DGPS for localization of its position, the follower was able to successfully track the delayed leader for 10 laps of the 1.3-kilometre track. A summary of the test results is shown in Table 1. The constant time delay was set to 8 seconds, and the look-ahead time was set to 3 seconds. The mean follower speed for the entire traverse was 2.2 m/s (7.9 km/h), and the mean following distance was 19 metres.

**Table 1** Summary of results from 10 laps of 1.3-kilometre track. The constant time delay was set to 8 seconds, and the look-ahead time was set to 3 seconds. The controller gains  $(k_{p,1}, k_{p,2}, k_{p,3}) = (0.08 s^{-1}, 0.04, 0.04)$ . The lateral error,  $\varepsilon_2$ , is calculated in the delayed leader’s frame, and  $t_f$  is the finishing time for the entire 13-kilometre traverse.

Description	Symbol	Value
Mean Follower Speed	$v$	2.2 m/s (7.9 km/h)
Mean Following Distance		19 m
Mean Lateral Error $\pm$ Standard Deviation	$\frac{1}{t_f} \int_0^{t_f} \varepsilon_2(q) dq$	0.07 m $\pm$ 0.46 m
Maximum Absolute Lateral Error	$\max_t  \varepsilon_2(t) $	2.73 m

**Fig. 8** The longitudinal and lateral errors,  $(\varepsilon_1, \varepsilon_2)$ , are in the delayed leader's frame, and the longitudinal and lateral errors,  $(e_1, e_2)$ , are in the follower's frame.



The mean lateral error was 0.07 metres with a standard deviation of 0.46 metres. The maximum absolute lateral error was 2.73 metres, which occurred during one of the turns at the hairpin. Since it is more natural to calculate an error with respect to the reference, the lateral errors here are calculated in the delayed leader's frame. The difference between tracking errors in the delayed leader's frame and tracking errors in the follower's frame is shown in Fig. 8.

Plots of DGPS ground truth data for a typical lap around the track are shown in Fig. 9. Figure 9a shows the leader's and follower's paths, while a close-up of the hairpin turn is shown in Fig. 9b. The longitudinal and lateral errors in the delayed leader's frame are shown in Fig. 9c, along with the delayed leader's and follower's speeds. The simultaneous large error increases around the 50-second and 400-second marks correspond to the U-turn and the hairpin turn, respectively. It should be noted that the longitudinal error did not get to zero during the 13-kilometre traverse. We have fixed this issue by adding an integral gain on the longitudinal error in the control law for the commanded speed. Unfortunately, due to time and weather

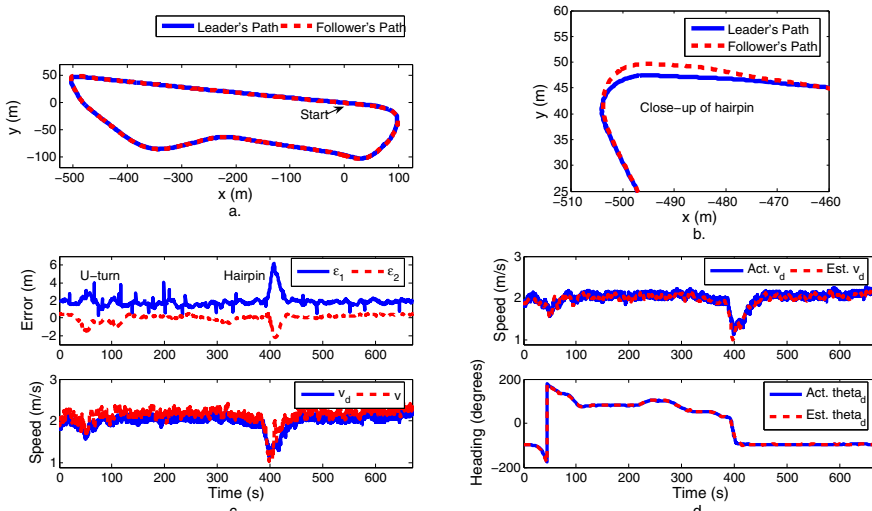


**Fig. 9** (a) The leader's and follower's paths. (b) A close-up of the paths during the hairpin (c) The longitudinal and lateral tracking errors, and the delayed leader's and follower's speeds. (d) The delayed leader's speed and heading compared with their estimates from windowing.

constraints, we have not been able to properly tune and test the follower with the improved controller. Since the longitudinal error was always positive and our control law is  $v_c = v_d + k_{p,1}e_1$ , the follower's speed was always slightly larger than the delayed leader's speed. However, because the follower deviated from the leader's path, it was never able to catch up to the delayed leader, resulting in its inability to reduce the longitudinal error to zero. In Fig. 9d, the delayed leader's actual speed and heading are compared with their estimates. The similarities of the plots suggest that windowing around  $t - \tau$  yields accurate speed and heading estimates.

## 4 Summary and Future Work

We have introduced the novel concept of tracking the trajectory of a vehicle ahead delayed by a constant time. This constant time delay forms the basis for our controller design and allows us to use ‘future’ position measurements to estimate the delayed leader’s speed and heading. Successful field trials were conducted with two full-sized vehicles over a 13-kilometre traverse in which the follower vehicle achieved a mean lateral error of 0.07 metres with a standard deviation of 0.46 metres.

For future work, we would like to perform vehicle-following experiments with odometry localization. We are confident that odometry localization will work with our approach as long as the odometric estimates are reasonably accurate over  $\tau$  (the constant time delay) seconds. To fix our poor heading estimate, we plan to implement a heading gyro on the follower. We would also like to conduct tests with multiple followers and at higher speeds. Testing multiple followers will provide us with important data on how tracking errors propagate in our system. To test at higher speeds, we plan to implement gain scheduling for our lateral controller since our lateral closed-loop system is dependent on the delayed leader’s speed. These tests will further validate the feasibility of our approach and will bring us closer to an operational autonomous convoy.

## References

1. Benhimane, S., Malis, E., Rives, P., Azinheira, J.R.: Vision-based control for car platooning using homography decomposition. In: Proceedings of the IEEE International Conference on Robotics and Automation, pp. 2161–2166 (2005)
2. Daviet, P., Parent, M.: Longitudinal and lateral servoing of vehicles in a platoon. In: Proceedings of the IEEE Intelligent Vehicles Symposium, pp. 41–46 (1996)
3. Franke, U., Bottiger, F., Zomotor, Z., Seeberger, D.: Truck platooning in mixed traffic. In: Proceedings of the Intelligent Vehicles Symposium, pp. 1–6 (1995)
4. Gehrig, S.K., Stein, F.J.: A trajectory-based approach for the lateral control of car following systems. In: IEEE International Conference on Systems, Man, and Cybernetics, vol. 4, pp. 3596–3601 (1998)
5. Giesbrecht, J.L., Goi, H.K., Barfoot, T.D., Francis, B.A.: A vision-based robotic follower vehicle. In: Proceedings of the SPIE Defence, Security, and Sensing, vol. 7332, pp. 14–17 (2009) (to appear)

6. Kehtarnavaz, N., Griswold, N.C., Lee, J.S.: Visual control of an autonomous vehicle (BART)—the vehicle-following problem. *IEEE Trans. on Veh. Tech.* 40(3), 654–662 (1991)
7. Marshall, J., Barfoot, T., Larsson, J.: Autonomous underground tramsing for center-articulated vehicles. *Journal of Field Robotics* 25(6-7), 400–421 (2008)
8. Schneiderman, H., Nashman, M., Wavering, A.J., Lumia, R.: Vision-based robotic convoy driving. *Mach. Vis. Appl.* 8, 359–364 (1995)
9. Swaroop, D., Rajagopal, K.R.: A review of constant time headway policy for automatic vehicle following. In: *Proceedings of the IEEE Intelligent Transportation Systems*, pp. 65–69 (2001)